This article has been accepted for publication in a future issue of this journal, but has not been fully edited. Content may change prior to final publication. Citation information: DOI 10.1109/TII.2022.XXXXXXX [TBC], IEEE Transactions on Industrial Informatics

Artificial Neural Network-Based Nonlinear Black-Box Modeling of Synchronous Generators

Mihailo Micev, *Student Member, IEEE*, Martin Ćalasan, *Member, IEEE*, Milovan Radulović, *Member, IEEE*, Shady H. E. Abdel Aleem, *Senior Member, IEEE,* Hany M. Hasanien*, Senior Member, IEEE*, Ahmed F. Zobaa*, Senior Member, IEEE*

***Abstract*— This paper deals with black-box modeling of synchronous generators based on artificial neural networks (ANN). ANN is applied to define the relationship between the excitation and terminal generator voltage values, while the Levenberg-Marquardt algorithm is used for determining the ANN's weight coefficients. The relation is made based on generator response on reference voltage step changes. The proposed approach is checked using the experimental results obtained from the measurements on a real 120 MVA generator from hydroelectric power plant Piva in Montenegro. Further, a fair comparison with the nonlinear auto-regression model with the exogenous input (NARX) and Hammerstein-Wiener (H-W) model is made. For the validation, different experiments were conducted – different values of step disturbances, other controller parameters, and different rotating speeds. Based on the presented results, it can be noted that the proposed ANN model is very accurate and provides a very high degree of matching with the experimental results and outperforms the other considered nonlinear models. Furthermore, the proposed test procedure and model is easy to implement and do not require disconnection of the generator from the grid or additional equipment for experimental realization. Such obtained models can be used for different testing types related to the excitation system.**

***Index Terms*— artificial neural networks, automatic voltage regulation, experimental measurements, Levenberg-Marquardt algorithm, nonlinear modeling, parameter identification, synchronous generators.**

I. Introduction

A. Background

SYNCHRONOUS generators (SGs) are one of the main parts of the entire electric power system sector. They are the largest producers of active power, but at the same time, they regulate the voltage level of the connection bus in the power system. Therefore, there are two control loops for the SG: turbine control used to maintain the frequency and active power at the desired level, and excitation control, which controls reactive power flow and voltage level. The analysis of the generator operation, both from the point of view of active power production or voltage regulation, requires an accurate and reliable model of the generator and an appropriate identification method [1]. This paper deals with the relation between the excitation and terminal generator voltage.

From the scientific point of view, the identification methods for SG parameters can be divided into time-domain and frequency-domain methods. The most important test methods from both groups, such as sudden-short circuit, load rejection, open-circuit, standstill frequency response, etc., are summarized in [2]. The time-domain methods comprise certain modifications of standardized test procedures [3]-[10], as well as the methods based on the phasor measurement unit (PMU) data [11]-[15]. Also, many researchers are dedicated to developing novel test procedures and methods for extracting the generator parameters, which are often based on certain modifications of Kalman filters [16]-[24]. In [25], the authors deal with the frequency-response identification method. All of the mentioned tests are described in detail in Section II.

The most comprehensive and accepted SG model is based on the Park's transformations. It relies on modeling the generator in a two-axis (d and q) frame.

B. Work motivation

The SG model presented with Park's transformations is a model composed of the two electrical circuits (one of the d-axis

and the other for the *q*-axis). These electrical circuits consist of many parameters (resistances, reactances, and corresponding time constants). In that way, the closed-form model of the SG can be obtained. Most of these parameters used to describe the generator can be determined only from the sub-transient and transient processes, which demand conducting very complicated experiments on the generator. To be more precise, these experiments require expensive equipment to provide the measurements with many samples with a small sampling time. The values of the Park's model parameters can be a few hundred times higher than the others, which may cause significant accuracy problems during the extraction process.

The significant characteristic of each identification method is whether the generator must be disconnected from the grid or the identification procedure can be carried out during the generator's normal operating mode. The disconnection of the generator can cause economic losses and problems with stability, reliability, and operation of the whole power system since the producing capacity is significantly reduced due to the removal of the generator. Therefore, so-called online methods, conducted while the generator operates on-grid, are highly desirable because they do not impact the global function of the power system. However, it should be noted that some of the existing online methods require information about some specific variables, such as power angle [26]. On the other side, the identification method should be conducted using the equipment already in the power plant. The need for the usage of additional equipment for the experiment only increases the overall cost of the experimental setup.

Starting from Park's model of the SG, the determination of the relationship between excitation and terminal voltage is very complex. It requires solving a set of highly complex differential equations. According to this, such an approach is time-consuming and inappropriate. Based on all previously discussed and noted facts, the necessity of research for a new approach for modeling the excitation voltage-terminal voltage relation is obvious.

C. Novelty and contributions

This paper focuses on black-box modeling of the relation between excitation voltage and the terminal voltage of the SG. Hence, in this paper, the output of the black-box model is the generator terminal voltage, while the input is the excitation voltage. The nonlinear black-box modeling of SGs contrasts with other well-known generator models. Black-box models are recently prevalent because they show a high degree of accuracy; they are easy to optimize and run very rapidly. Also, these models do not require high computing power [27]. The black-box models only aim to provide the mapping of output and input of the model without knowing and understanding the model's behavior.

In this paper, we propose black-box modeling of the SG using artificial neural networks (ANNs). Based on the authors' knowledge, this is the first time such a modeling approach has been presented. The ANNs are very popular because of their numerous advantages, among which the most important is the ability to learn and model both linear and non-linear complex relations. Also, the ANNs have high generalization ability, making them very applicable for modelling unseen relations and data. Furthermore, the application of the ANN as the controller instead of the conventional PI controller in the AVR system significantly improves the system's dynamic response [28]. Moreover, ANNs can work even when input and output data are corrupted, *i.e.*, noisy data or missing data samples [29,30].

Therefore, the main paper contributions are outlined as follows:

- The novel modeling approach, which maps the excitation and terminal voltage of the SG, is proposed.
- The novel identification test procedure, which does not require the disconnection of the SG, is demonstrated. This test procedure introduces a small step disturbance on the reference generator voltage and measures the excitation and terminal voltage waveforms.
- The proposed identification procedure is applicable for both on-grid and off-grid generator operation modes.
- The validation is provided on a real 120 MVA SG from the hydropower plant (HPP) Piva in Montenegro.
- The application of the ANN model is superior compared to other literature known nonlinear models, such as the nonlinear auto-regression model with exogenous input (NARX) and Hammerstein-Wiener (H-W) models. Note, black-box modeling of the SG using the NARX model is presented in [12], but without experimental testing on a real, large-power SG.
- The proposed approach is generic, which means it can be applied to SGs of different power and voltage level.

D. Paper organization

This paper is organized as follows. Section II provides details about the existing methods for determining SG parameters. In Section III, a brief description of neural networks is presented. Afterward, Section IV describes the test procedure for identifying neural network weight coefficients. As depicted in Section V, the real validation is provided with the experimental testing of the proposed method on a real SG. Section VI presents the validation through the simulations. The final concluding comments of this work are given in the Conclusion section.

II. Related works

This section presents a brief overview of the recently proposed identification methods of SG parameters. Regarding the existing test procedures for determining SG parameters, the most relevant ones are sublimed in [2]. The modifications of the standardized test procedures are presented in [3]-[10]. Three modified standard tests are combined to determine SG parameters in [3]. The load rejection test is applied to SGs in [4] and [5], where the parameters are extracted by the interior point method [4] and the graphical method [5]. The research presented in [5] expands the load rejection test to consider the

This article has been accepted for publication in a future issue of this journal, but has not been fully edited. Content may change prior to final publication. Citation information: DOI 10.1109/TII.2022.XXXXXXX [TBC], IEEE Transactions on Industrial Informatics

effect of saturation. Furthermore, the short-circuit test has been presented in [6], considering field voltage variations. The authors in [7] and [8] identified the SG's parameters using simplified analytical waveforms of the field and armature short-circuit current, respectively. In [9], the simplified expressions are substituted by the full field and armature current expressions, which do not neglect any parameter of the generator, and therefore it needs to be expressed by the inverse Laplace transformation. Different tests are demonstrated in [10] – short-circuit test along with decrement of field, slip test, and voltage test. Unfortunately, despite the presence of standardized tests, many authors insist on developing non-standardized test procedures for determining the generator's parameters.

It is worth mentioning the methods that use the data obtained from the PMU (active and reactive power, voltage magnitude, and phase) for identifying the generator parameters [11]-[15]. Additionally, the identification methods presented in [16]-[19] are based on applying different signals to the stator windings while the field winding is short-circuited. The signals that can be applied to the stator windings are Pseudo-Random Binary Sequence (PRBS) [16], chirp signal [17], sine cardinal signal [18], and step signal [19]. The previously presented methods have a significantly higher cost since the PMUs and the equipment needed for generating the different signals are expensive. The identification method presented in [20] defines the load conditions required to obtain pure *q*-axis armature current and therefore determine *q*-axis parameters. Specific current and voltage waveforms during the power system's remote line-to-line fault can be used to determine the generator parameters, as depicted in [21]. The authors in [22] proposed an efficient three-stage algorithm for identifying the turbine-governor and SG parameters using their precise models. The Unscented Kalman Filter (UKF) application to estimate the parameters of the SG during unbalanced operating conditions is presented in [23]. In [24], the Constrained Iterative Unscented Kalman Filter (CIUKF) is used to determine the generator parameters using the data obtained by a digital protective relay (DPR).

Unlike the time-domain methods, the original standstill frequency response (SSFR) test and its modifications [25] generate multiple sinusoidal voltages with various frequencies. Therefore, the frequency-domain tests are somewhat complicated, time-consuming, and require complex mathematical analysis. Due to this, the time-domain tests are more applicable than the frequency-domain tests.

III. Artificial Neural Networks

ANNs are trendy computational modeling facilities that have recently engaged in many applications. They can be explored as complex structures consisting of interconnected adaptive simple processing elements and artificial neurons. ANNs represent the analogy with the human nervous system, whose basing building block is the biological neuron (dendrites, cell body, and axon). The dendrites collect signals from other neurons and send them to the cell body. Afterward, the axon gets signals from the cell body and transfers them to other neurons through the synapse. Since each neuron has many dendrites and synapses, it can transmit many signals simultaneously. Such a mechanism represents the basis that led to the creation and development of ANNs. Fig. 1 illustrates a straightforward system of artificial neurons – a system of biological neurons.

In Fig. 1, *n* denotes the number of neurons, and *x* and *w* denote the intensity and synaptic strengths, respectively [29]. Mathematically, *n* denotes artificial neurons, x_i represents the input signals, *w* stands for weight coefficients, and *y* represents the output signal.

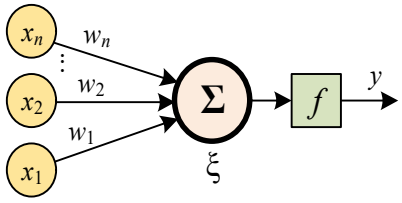

Fig. 1. System of artificial neurons.

The linear combination of input signals is fed into the neuron whose *b* is its threshold or bias. When $\xi = \sum_{i=1}^{N} w_i x_i$ exceeds *b*, the neuron becomes activated, which can be mathematically expressed as follows [29]:

$$y = f(\xi) = \begin{cases} 1, & \xi \geq b \\ 0, & \xi < b \end{cases} \tag{1}$$

where *f* is called the activation function; in this case, the activation function is the well-known step function. Alternatively, in the literature, the neuron threshold might function as an additional input node whose value is *x*=1 and weight coefficient *w*=*b*.

In order to be able to deal with nonlinear problems, the simple neural network presented in Fig. 1 is expanded with more additional layers of neurons, which are located between the input and the output layers. The intermediate layers are so-called hidden layers. In this way, a multi-layer neural network or multi-layer perceptron (MLP) network is obtained. The neurons from the hidden layer receive the information from input neurons, process them, and forward them to the output layer. The structure of a multi-layer network with four input neurons, three neurons in a hidden layer, and two output neurons is illustrated in Fig. 2.

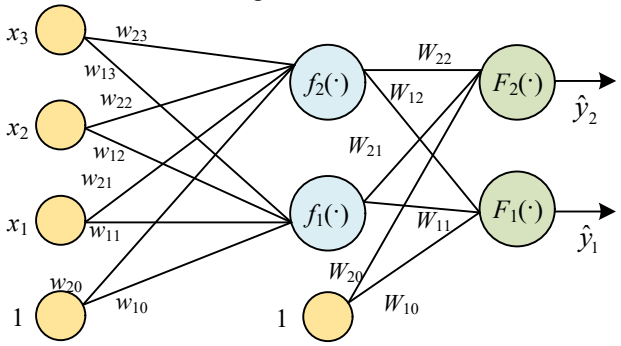

Fig. 2. The structure of a 3-layer MLP.

According to Fig. 2, the output y_i (i={1,2}) of the neural network can be represented as follows [29,30]:

$$y_i(\boldsymbol{w},\boldsymbol{W}) = F_i\left(\sum_{j=1}^{q} W_{ij} f_j\left(\sum_{k=1}^{m} w_{jk} x_k + w_{k0}\right) + W_{i0}\right) \quad (2)$$

where q denotes the number of neurons in the hidden layer, while m denotes the number of inputs, and the activation functions are denoted as F and f. The weight coefficients, specified by the matrices $\boldsymbol{w}$ and $\boldsymbol{W}$, are adjustable parameters of the network obtained throughout the process named training of the network. The training procedure is carried out with the help of the training data, which consists of a set of inputs $u(t)$ and the corresponding desired outputs $y(t)$. If the training set is denoted Z^N, it can be formulated as follows:

$$Z^N = \left\{\left[u(t), y(t)\right]; t = 1, 2, ..., N\right\} \quad (3)$$

where N stands for the number of samples, the training process aims to decide the weights $\boldsymbol{w}$ and $\boldsymbol{W}$ so the outputs of the neural network, also called predicted outputs, $\hat{y}(t)$, are likely close to the real outputs $y(t)$.

The prediction error strategy used in this paper is based on determining the weight coefficients, so the mean-square-error function (V_N) is minimized [30], thus:

$$V_N\left(\boldsymbol{w},\boldsymbol{W},Z^N\right) = \frac{1}{2N}\sum_{t=1}^{N}\left[y(t) - \hat{y}(t,\boldsymbol{w},\boldsymbol{W})\right]^T \left[y(t) - \hat{y}(t,\boldsymbol{w},\boldsymbol{W})\right] \quad (4)$$

In this work, the weight coefficients are determined by the modified Levenberg–Marquardt (LM) algorithm, which is very popular for solving nonlinear least-squares problems. This algorithm is an iteration-based algorithm, where the weight coefficients, summarized in vector θ, are updated as expressed in (5).

$$\theta^{(i+1)} = \theta^{(i)} + f^{(i)} \quad (5)$$

where i stands for the current iteration and f denotes the search direction.

This algorithm combines two numerical minimization algorithms: the gradient descent method and the Gauss-Newton (GN) method. The LM method behaves like a gradient–descent method when the parameters are far from their optimal values, while it behaves like the GN method when the parameters are close to the optimal value. The behavior of the LM algorithm is defined by the ratio between actual and predicted lessening of the fitness function V_N, denoted as $r^{(i)}$. Thus;

$$r^{(i)} = \frac{V_N\left(\theta^{(i)}, Z^N\right) - V_N\left(\theta^{(i)} + f^{(i)}, Z^N\right)}{V_N\left(\theta^{(i)}, Z^N\right) - L^{(i)}\left(\theta^{(i)} + f^{(i)}\right)} \quad (6)$$

where L is expressed as follows:

$$L^{(i)}\left(\theta^{(i)} + f^{(i)}\right) = \sum_{t=1}^{N}\left(y(t) - \hat{y}\left(t,\theta^{(i)}\right) - f^T \frac{\partial \hat{y}(t,\theta)}{\partial \theta}\Big|_{\theta=\theta^{(i)}}\right)^2 \quad (7)$$

By introducing G as the gradient of the fitness function V_N with respect to the weights θ, and R as the GN approximation of the Hessian:

$$G = \frac{\partial V_N\left(\theta, Z^N\right)}{\partial \theta}$$
$$H = \frac{1}{N}\sum_{t=1}^{N}\frac{\partial\left(y(t) - \hat{y}\left(t,\theta^{(i)}\right)\right)}{\partial \theta}\left(\frac{\partial\left(y(t) - \hat{y}\left(t,\theta^{(i)}\right)\right)}{\partial \theta}\right)^T \quad (8)$$

Hence, (7) can be rewritten as follows:

$$L^{(i)}\left(\theta^{(i)} + f^{(i)}\right) = V_N\left(\theta^{(i)}, Z^N\right) + f^T G\left(\theta^{(i)}\right) + \frac{1}{2} f^T R\left(\theta^{(i)}\right) f^T \quad (9)$$

The steps of the LM algorithm are given as follows:

1) Initialize the values of weight coefficients $\theta^{(0)}$ and step size $\lambda^{(0)}$.
2) Govern the search direction f from the following expression:

$$\left[R\theta^{(i)} + \lambda I\right] f^{(i)} = -G\left(\theta^{(i)}\right) \quad (10)$$

where I denotes the unity matrix.

3) Calculate the value of ratio $r^{(i)}$ using (6) to determine the search direction approach:
- If $r^{(i)} > 0.75 \Rightarrow \lambda^{(i)} = \lambda^{(i)}/2$ – the foreseen reduction of the fitness function value is close to the actual decrease, which means the LM algorithm should behave as a GN algorithm.
- If $r^{(i)} < 0.25 \Rightarrow \lambda^{(i)} = 2\lambda^{(i)}$ – the foreseen reduction of the fitness function value is far from the actual decrease, and therefore the LM algorithm should act as a gradient descent algorithm.

4) Update the vector of weight coefficients $\theta^{(i+1)} = \theta^{(0)} + f^{(i)}$ and increase the iteration counter: $i = i + 1$.
5) Check the stopping criterion, and if it is not met, return to step 2). If it is met, the obtained vector θ holds the optimal values of the weight coefficients.

IV. Identification Procedure

As stated previously, the neural network is trained, *i.e.*, the weight coefficients are determined with the help of training set data. Training set Z^N comprises a set of inputs $u(t)$ and corresponding outputs $y(t)$. Considering that the neural network is used to model the SG in this paper, the input signal u for the neural network is the excitation voltage V_f of the generator, while the output signal of the neural network y is the voltage at the generator's terminals V_t.

The input-output dataset, represented by the excitation and the generator's terminal voltage, is experimentally obtained during the no-load operation mode of a real SG (120 MVA, 15.75 kV) in a hydroelectric power plant (HPP) Piva in Montenegro. The photo of the SG used for experiments done in this work is presented in Fig. 3. The experimental tests and the measurements of the voltage waveforms were realized in July 2020. The excitation system of this generator is the static excitation system UNITROL 6000, which is realized as a self-excited thyristor-controlled system manufactured by ABB. This system provides the excitation voltage to the generator's field winding and enables safe and secure control of all variables. The microprocessor technique realizes the control of the system. The block diagram of the AVR system used for the 120

This article has been accepted for publication in a future issue of this journal, but has not been fully edited. Content may change prior to final publication. Citation information: DOI 10.1109/TII.2022.XXXXXXX [TBC], IEEE Transactions on Industrial Informatics

MVA SG voltage regulation is given in Fig. 4.

Fig. 3. The used SG in the experiments in HPP Piva.

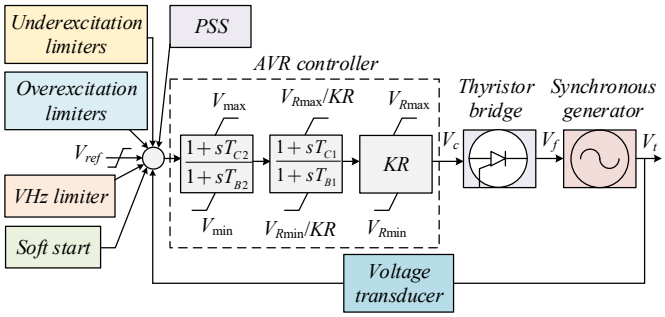

Fig. 4. The block diagram of the experimental setup.

The controller in the AVR system is realized as a combination of lead-lag compensators, including anti-windup protection and proportional gain *KR*. The values of the controller parameters are: T_{C1}=3.5, T_{B1}=11.67, T_{C2}=0.1, T_{B2}=0.1, KR=500, $V_{R\min}$=−6.4, $V_{R\max}$=7.27, $V_{\min}$=−0.0912, $V_{\max}$=0.0912. The error signal, which represents the input to the controller, is formed from many different signals: reference voltage, measured terminal voltage, power system stabilizer (PSS) signal, a soft start signal, V/Hz limiter signal, and signals from overexcitation and under-excitation limiters. Under-excitation limiters include a PQ limiter that prevents the generator from operating beyond practical stability limits, a minimum field current limiter and a capacitive stator current limiter. Overexcitation limiters comprise the maximum field current limiter and inductive stator current limiter. The AVR controller defines the control signal V_c based on the error signal, which is converted to the thyristor bridge control angle (α).

The experiments conducted for this paper comprise the SG and the AVR system of the generator. The central role of the AVR system is to keep the voltage at the generator's terminals at the desired value, which is dictated by the reference voltage signal V_{ref}, which represents the input of the AVR system. The test procedure for identifying the neural network weight coefficients consists of measuring the field and the generator's terminal voltage when there are step changes in the reference voltage value of the AVR system. Such described test procedure can produce the dynamic processes of the generator, but does not impact the normal operation of the power system in terms of active power injection. The complete block diagram of the test procedure applied in this paper is depicted in Fig. 5.

Precisely, the experimental measurements for obtaining the dataset for neural network training are carried out by setting the AVR system reference voltage at the rated value (1 p.u, where p.u stands for per unit). Afterward, the reference voltage is reduced by 5% to 0.95 p.u, while after a particular time, it gets increased to the final value of 1.05 p.u. During such operation mode, which is very safe for the generator itself and the whole power system, the excitation and terminal voltage are measured and serve as the training dataset. The measured excitation voltage is given in Fig. 6, while the generator terminal voltage and the reference voltage are depicted in Fig. 7. The exact values of experimental measurements for some samples are given in the Appendix. Also, the flowchart of the ANN training procedure is depicted in the Appendix.

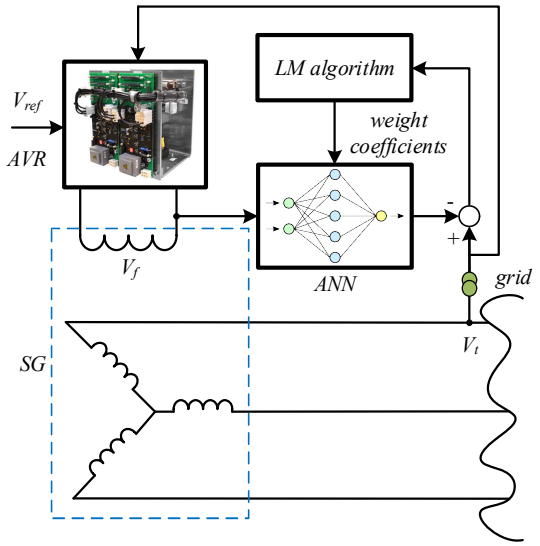

Fig. 5. Complete block diagram of the proposed identification procedure.

V. Experimental Results

The voltage waveforms represented in Figs. 6 and 7, as stated before, serve as the input-output dataset for the training of neural networks using the described LM algorithm.

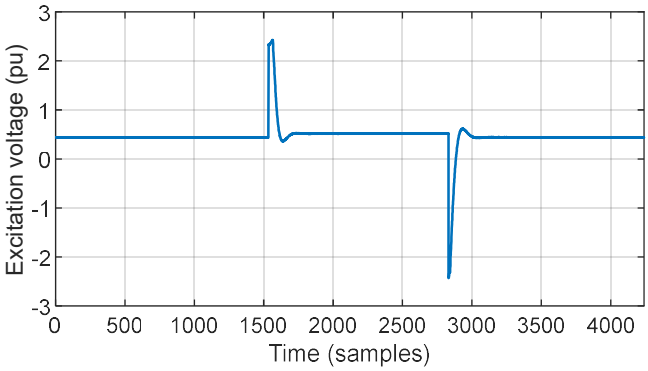

Fig. 6. Experimental excitation voltage – input training data.

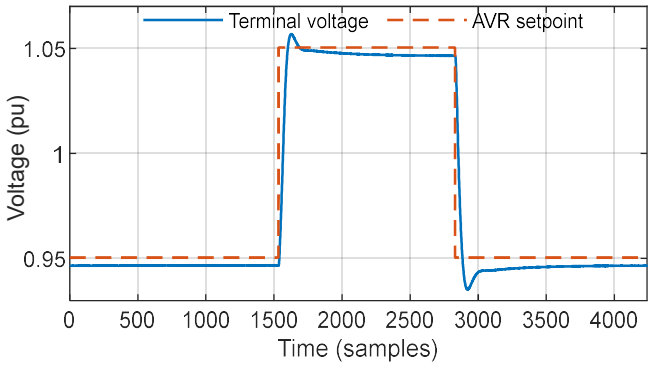

Fig. 7. Experimental terminal voltage – output training data.

This paper uses the ARX (auto-regression model with the exogenous input) architecture of the neural network. It means that the neural network inputs are past values of input and output data, i.e., excitation and terminal voltage. The neural network used in this work has four neurons in the input layer, which means the inputs are two past values of input and output data: $u(t-2)$, $u(t-1)$, $y(t-2)$, $y(t-1)$. Additionally, there is one bias neuron in the input layer, denoted with "1" in Fig. 2. The hidden layer consists of five neurons, with an additional bias neuron, as in the input layer. The activation function for the hidden layer is hyperbolic tangents, *i.e.*, f=tanh. The output layer consists of one neuron, whose activation function F is linear.

The neural network training process stands for the determination of the weight coefficients $\boldsymbol{w}$ (from input to hidden layer) and $\boldsymbol{W}$ (from hidden to output layer) with the help of the training algorithm and the criterion function defined with (4). The training algorithm stops when any criterion of the following stoppings criteria is met – (i) the maximum number of iterations, which is set to 500 in this work, is reached, (ii) the value of criterion function (4) drops below criterion minimum value, which is equal to 0, and (iii) change of the criterion function is below 10^{-7}, the gradient's largest element is below 10^{-4}, and the most prominent change of weight coefficients is below 10^{-3}. In this paper, several training algorithms are implemented and mutually compared: Levenberg-Marquardt (LM), back-propagation (BP), an incremental version of the back-propagation algorithm, and iterated generalized least squares (IGLS) algorithm. All algorithms are applied under the same stopping condition, which is previously defined. The mentioned algorithms are compared in terms of the execution time, obtained criterion function (CF) value, and the number of iterations, as given in Table I.

TABLE I
COMPARISON OF THE ANN TRAINING ALGORITHMS

Algorithm	LM	BP	INCBP	IGLS
Time (s)	**< 1**	< 1	35	~ 2
CF value	**2.8765×10^{-8}**	2.652×10^{-4}	6.1×10^{-4}	2.88×10^{-8}
Iterations	**167**	500	500	188

Based on the results presented in the previous table, it is evident that the LM algorithm is superior compared to the other frequently applied training algorithms. For that reason, in this paper, the LM algorithm is applied for training the neural network. The convergence curve – the values of the criterion function after each iteration – is depicted in Fig. 8.

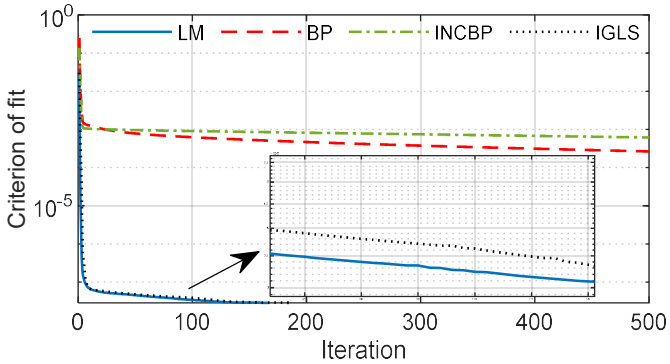

Fig. 8. Convergence curves of compared training algorithms.

The weight coefficient $\boldsymbol{w}$ is obtained as a 5×5 matrix, while the weights $\boldsymbol{W}$ are given in a row vector of 6 elements, as shown below.

$$\boldsymbol{w}=\begin{bmatrix} 0.255 & 0.191 & -2.9e-4 & -0.0157 & -0.079 \\ -0.36 & -0.209 & 0.001 & 0.002 & 0.19 \\ -0.03 & 0.003 & 0.1543 & 0.137 & -0.061 \\ -0.33 & -0.204 & 0.005 & -0.002 & 0.128 \\ 0.364 & 0.203 & -0.006 & 0.005 & -0.168 \end{bmatrix}, \quad (11)$$

$$\boldsymbol{W}=\begin{bmatrix} 0.446 & -0.588 & 0.041 & -0.543 & 0.582 & 0.202 \end{bmatrix}.$$

A graphical comparison of the terminal voltage obtained by the trained neural network and the experimentally measured voltage is depicted in Fig. 9.

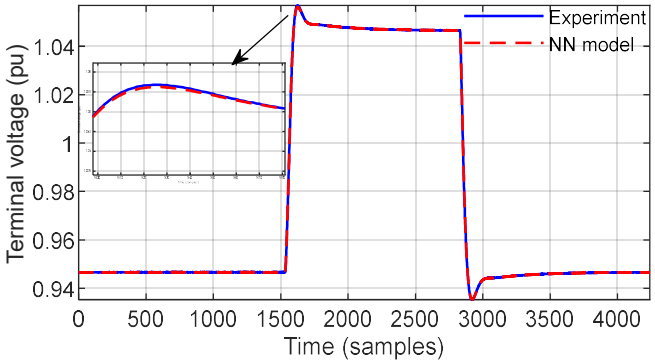

Fig. 9. Graphical comparison of ANN voltage and the voltage used for training.

After the training process is completed, it is crucial to validate such a trained neural network. For that purpose, four different experiments are carried out, and the corresponding excitation and terminal voltage waveforms are measured:

1) **Validation 1** – step disturbances on the reference voltage value are the same as in Fig. 6 (0.95 p.u-1.05 p.u- 0.95 p.u), but the parameters of the AVR controller are reduced.

2) **Validation 2** – step disturbances on the reference voltage value are varied: at the beginning, the reference voltage is 1 p.u, afterward, it drops to 0.97 p.u, and finally, it is set to 1.03 p.u; parameters of the controller are settled at the normal value.

3) **Validation 3** – reference voltage is the same as validation test 1 (0.95 p.u-1.05 p.u-0.95 p.u), controller parameters are at

the normal value, but the rotating speed is reduced to 90% of the rated speed.

4) **Validation 4** – the reference voltage remains the same as in the previous test, speed is at 90% of the rated value, but the controller parameters are reduced.

The validation of the neural network is carried out by comparing the terminal voltage obtained by the neural network with the corresponding experimentally recorded voltage waveform. Furthermore, the proposed neural network (NN)-based model is compared with the NARX [12] and Hammerstein-Wiener (H-W) models. The error signals are shown for each validation test. Figs. 10-13 depict the results of the validation tests, respectively.

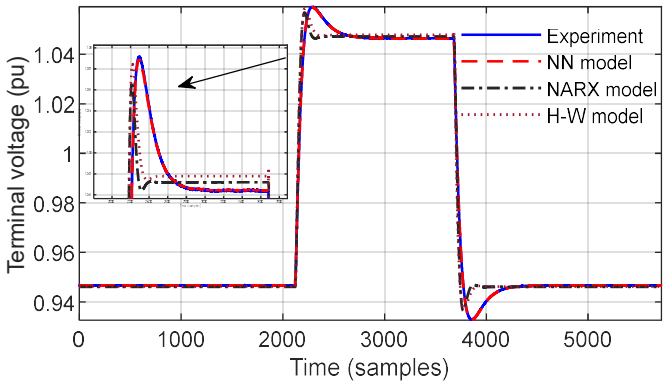

(a)

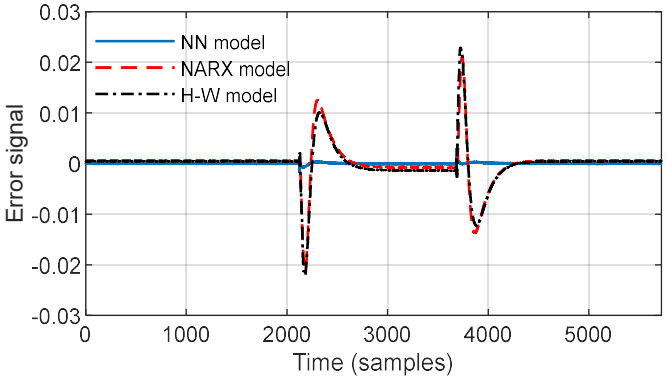

(b)

Fig. 10. Validation test 1: (a) Graphical comparison of the voltage waveforms, and (b) Error signals.

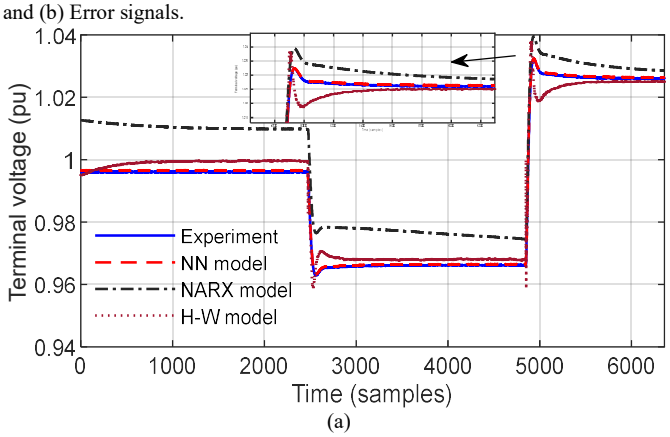

(a)

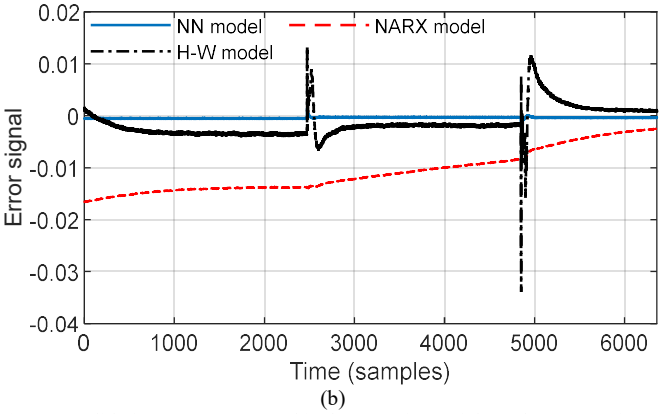

(b)

Fig. 11. Validation test 2: (a) Graphical comparison of the voltage waveforms, and (b) Error signals.

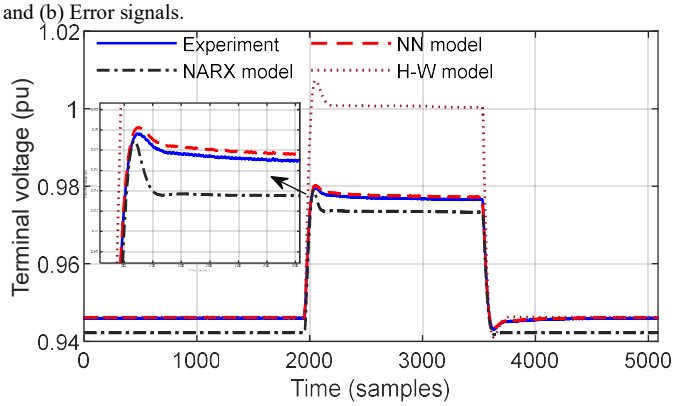

(a)

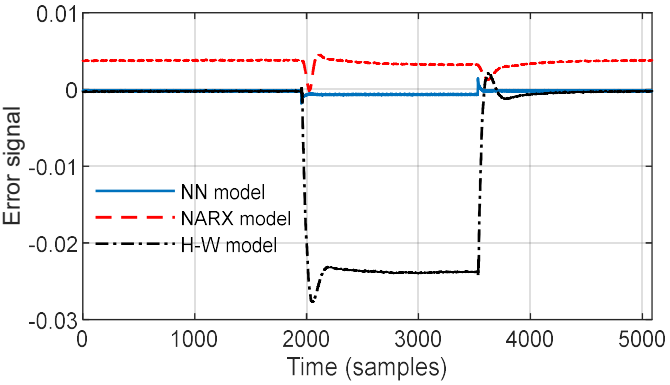

(b)

Fig. 12. Validation test 3: (a) Graphical comparison of the voltage waveforms, and (b) Error signals.

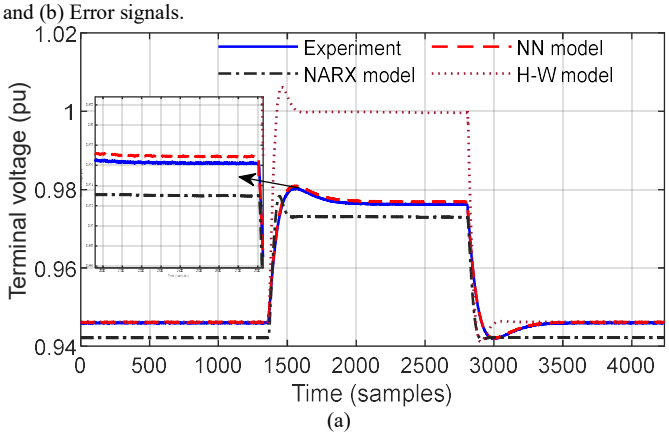

(a)

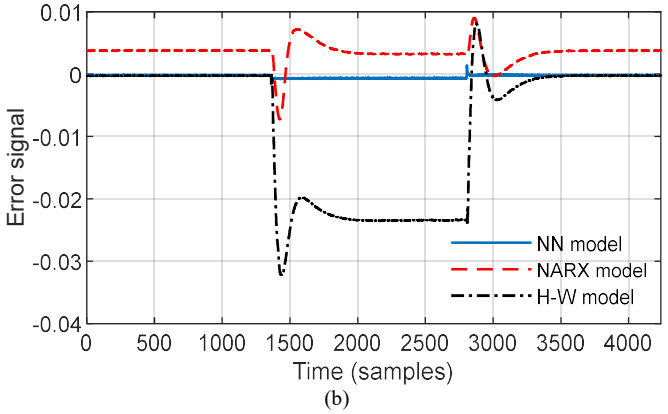

(b)

Fig. 13. Validation test 4: (a) Graphical comparison of the voltage waveforms, and (b) Error signals.

One significant additional advantage of using the ANN model is its simplicity and computational speed compared with the other two considered models, NARX and H-W. The time required to train the neural network and the time to estimate the NARX and H-W model parameters are depicted in Table II.

TABLE II
TIME COMPLEXITY COMPARISON OF USED MODELS

Model	ANN	NARX	H-W
Time (s)	< 1	7.4	10

The neural network training is practically instantaneous and takes less than 1 second to be completed. Estimating NARX and H-W model parameters is much slower, and it can take around 7 seconds for NARX and approximately 10 seconds for the H-W model. It is essential to mention that the accuracy and precision of NARX and H-W models are strictly dependent on the order of these models. Lower orders of these models result in inadequate and inaccurate results, which are not presented in the manuscript. In order to obtain any results that are even close to the experimental ones, we had to adopt NARX and H-W models of a very high order. This fact makes these two models very complex, and therefore there are a large number of the parameters of these models which need to be estimated.

To sum up, all of the validation tests represent different operating conditions of the excitation system of the SG. The previously presented figures depict the graphical comparison of experimentally recorded voltage with the generator voltage waveforms obtained by the ANN, NARX, and H-W models, respectively.

Despite the graphical comparison, the degree of matching between experimental voltage and the voltage obtained from the models can be expressed with the error signal $e=V_{exp}-V_{model}$, where V_{exp} stands for the experimentally obtained voltage, and V_{model} denotes the voltage calculated by the ANN, NARX, or H-W model. The more precise and accurate model is the one whose error signal has the lowest values. The generator's voltage obtained by the trained neural network closely matches the experimentally obtained voltage, proven by the graphical comparison of the voltage waveforms. For all the presented validation tests, the error between experimental and ANN voltage waveforms is lower than 0.1% in the steady-state.

Relying on the results presented, it was evident that the proposed black-box nonlinear ANN-based modeling of the SG is very accurate for different conditions, particularly in the presence of the AVR system. It was also clear that the accuracy and precision of the proposed approach are much higher than the literature-known NARX and H-W models. As seen in the previous figures, the terminal voltage calculated by the NARX and H-W models cannot reach the steady-state reference value. Besides, the accuracy in the transient period is also significantly lower (worse) than the voltage obtained by the proposed ANN model. Additionally, it was also proven that the ANN model is considerably less time-consuming since the time required to train the ANN is drastically lower than the time required to estimate NARX and H-W model parameters. Therefore, it can be concluded that the proposed model of the SG can be very applicable in practice. Such an SG model can be applied for different tests related to the safe operation of SG, including examination of field overexcitation and demagnetization, and others.

VI. SIMULATION RESULTS

The modeling approach introduced in this paper is generic, *i.e.*, it is applicable not only for a single SG used in experiments but also for various generators with different rated power and rated voltage. In order to confirm this, the ANN model of the SG is verified with simulations conducted in MATLAB Simulink software on a 40 MVA, 10.5 kV SG from HPP Perucica in Montenegro. Also, a comparison with NARX and H-W models is provided. After the corresponding Simulink model is developed, the excitation voltage, which also represents the input training data for the ANN, is applied to the field winding of the SG. In this case, the excitation voltage is defined as the PRBS signal, and the generator terminal voltage, which serves as the output training data, is recorded. The input and output training data are depicted in Fig. 14.

After proper training of the neural network, whose structure is the same as the one from the previous section, the output of such network should be compared with the output training data. Therefore, a graphical comparison of the terminal voltage obtained by the trained neural network and the voltage recorded from the Simulink model is depicted in Fig. 15.

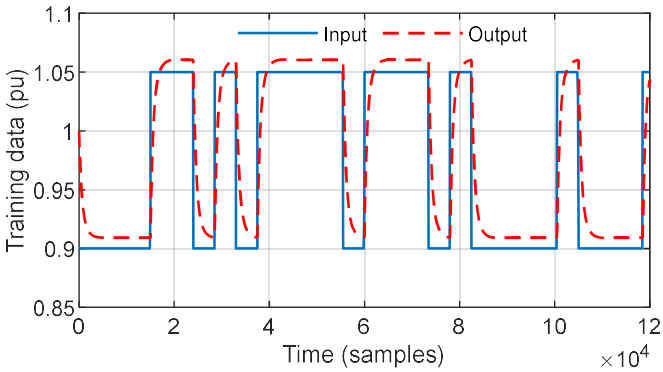

Fig. 14. Input and output training data.

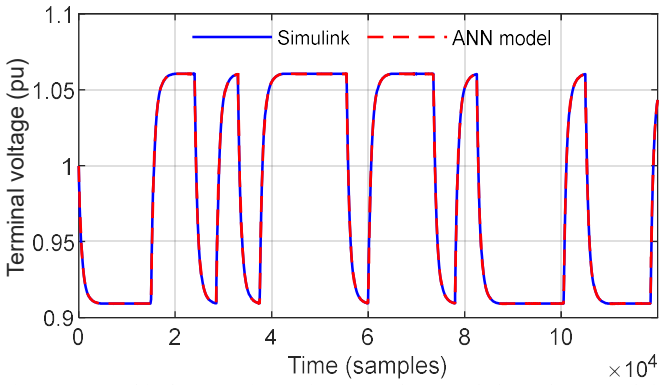

Fig. 15. Graphical comparison of ANN voltage and the voltage used for training.

The validation test is carried out by defining the input signal as the PRBS signal whose pulse width is less than the one used for training. The input and output validation data are depicted in Fig.16. Based on such a defined input signal, the outputs of the trained ANN and identified NARX and H-W models are calculated and compared with the obtained terminal generator voltage from the Simulink model (output validation data). The graphical comparison of these voltage waveforms and the error signal are depicted in Fig. 17.

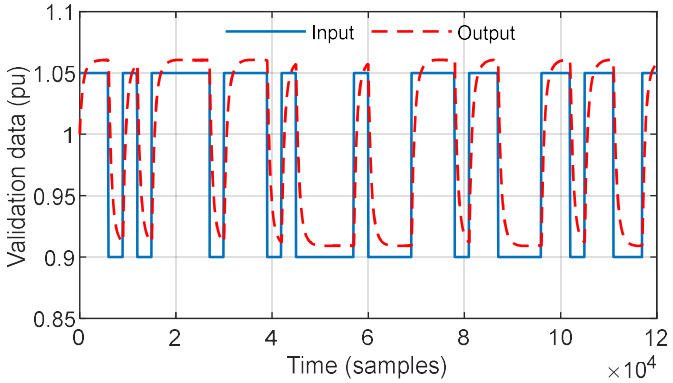

Fig. 16. Input and output validation data.

Observing the presented results, it is obvious that the voltage of the generator obtained by the ANN model matches perfectly with the corresponding voltage recorded from the Simulink model of the SG.

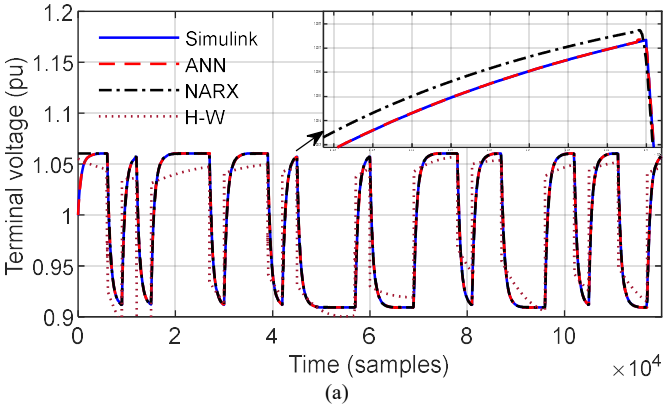

(a)

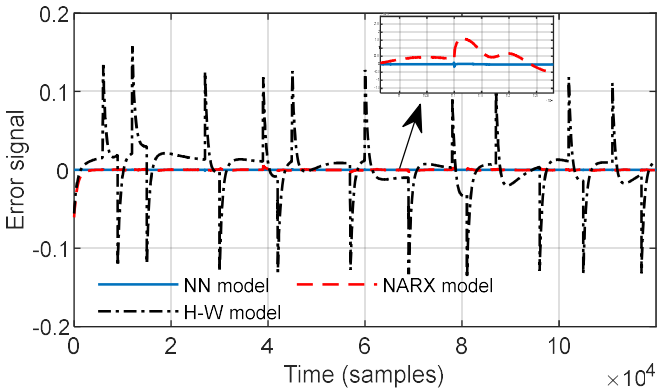

(b)

Fig. 17. Validation test: (a) Graphical comparison of the voltage waveforms, and (b) Error signals.

Once again, it is proven that the ANN model is extremely precise and accurate for modelling the relationship between excitation and the terminal voltage of the generator, even when a different type of excitation voltage signal is applied. Also, the superiority of the ANN model in comparison with NARX and H-W models is proven again.

VII. Conclusion

In this article, an ANN-based model of an SG is presented. The neural network is trained with the Levenberg-Marquardt algorithm, where the excitation voltage represents the input training data, and the generator terminal voltage stands for the output training data. The proposed test procedure measures the excitation and terminal voltage waveforms when there are step disturbances on the AVR system setpoint. During the described test, the generator remains in its' normal on-grid operation mode, making it very easy to conduct. Furthermore, the validation of the neural network was carried out with the experimentally obtained results on a real 120 MVA SG in hydropower plant Piva in Montenegro, as well as with the results obtained using the NARX and H-W models presented in the literature. Also, the simulation analysis for a 40 MVA SG from hydropower plant Perucica is provided. The output voltage of the neural network well matches the corresponding experimentally obtained voltage, which indicates that the neural network-based model of the generator is precise, accurate, and applicable. Since all of the four validation tests were carried out during different operating conditions of the AVR system, it can be deduced that the proposed neural network model can represent the generator regardless of the operating conditions of the power system. Much attention will be paid to extending the proposed ANN model for different active power values injected into the grid in future works. Besides, we will analyze the potential applications of such models in determining the optimal parameters of the AVR controller.

Appendix

The experimentally recorded excitation and terminal voltage from Figs. 6 and 7, which are used for training the ANN in this paper, are presented in Table III. Due to a large number of samples, we provided only some of them. Additionally, the

flowchart of the ANN training process is depicted in Fig. 18.

TABLE III
EXPERIMENTALLY MEASURED RESULTS

Sample	V_f (pu)	V_t (pu)	Sample	V_f (pu)	V_t (pu)
1	0.4418	0.947	2200	0.5143	1.047
250	0.4402	0.947	2400	0.5128	1.047
500	0.4435	0.947	2600	0.5163	1.047
750	0.4384	0.947	2800	0.5141	1.047
1000	0.4421	0.947	2820	0.5156	1.046
1250	0.4394	0.947	2840	-2.3106	1.033
1500	0.4428	0.947	2860	-1.1204	0.986
1515	0.4366	0.947	2880	-0.1539	0.955
1530	0.4395	0.947	2900	0.3843	0.939
1545	2.3433	0.959	2920	0.5859	0.935
1560	2.4133	0.987	2940	0.6033	0.937
1575	1.8889	1.017	2960	0.5566	0.940
1590	1.1195	1.040	2980	0.4976	0.942
1605	0.6637	1.052	3000	0.4564	0.943
1620	0.4365	1.056	3020	0.4382	0.944
1635	0.3625	1.056	3040	0.4331	0.944
1650	0.3792	1.055	3060	0.4346	0.944
1665	0.4225	1.053	3080	0.4372	0.944
1680	0.4658	1.051	3100	0.4407	0.944
1695	0.4933	1.050	3120	0.4415	0.944
1710	0.5124	1.049	3140	0.4426	0.945
1725	0.5231	1.049	3160	0.4415	0.945
1740	0.5251	1.049	3180	0.4424	0.945
1755	0.5177	1.049	3200	0.4419	0.945
1770	0.519	1.049	3400	0.4402	0.946
1785	0.52	1.049	3600	0.4403	0.946
1800	0.51740	1.049	3800	0.4395	0.946
2000	0.51820	1.048	4000	0.4404	0.947

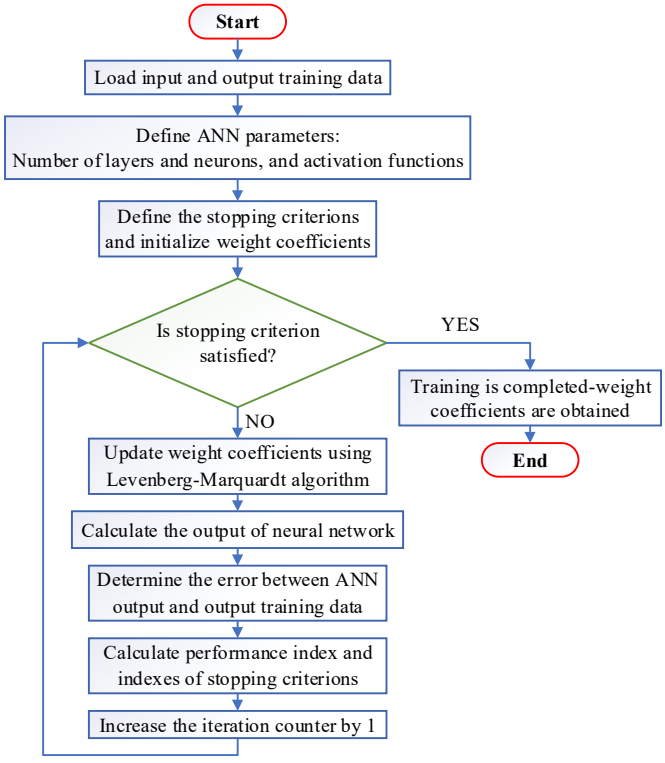

Fig. 18. Flowchart of the ANN training process.

The complete experimental measurements presented in Figs. 6 and 7, along with some of the used Matlab codes and Simulink models, are located on the following link: https://drive.google.com/file/d/1OlNfo56-QIgJUaKioGhenOJ28WNt88y3/view?usp=sharing. It can be downloaded with the permission of the authors.

REFERENCES

[1] T. A. Lipo, *Analysis of Synchronous Machines*, 2nd ed. Boca Raton, Florida, USA: CRC Press, 2017.

[2] *IEEE Guide: Test Procedures for Synchronous Machines*, IEEE Standard 115-1995, 1995.

[3] M. Ben Slimene, A. Salah Saidi, and M. A. Khlifi, "Estimation of Hydropower Synchronous Generator Parameters Through Field Simulations of Modified Standard Tests," *J. Electr. Eng. Technol.*, vol. 16, no. 1, pp. 91–99, 2021, doi: 10.1007/s42835-020-00575-7.

[4] G. Gutiérrez Rodríguez, A. Silveira e Silva, and N. Zeni, "Identification of synchronous machine parameters from field flashing and load rejection tests with field voltage variations," *Electr. Power Syst. Res.*, vol. 143, pp. 813–824, 2017, doi: 10.1016/j.epsr.2016.08.025.

[5] B. Zaker, G. B. Gharehpetian, and M. Karrari, "Improving Synchronous Generator Parameters Estimation Using $d- q$ Axes Tests and Considering Saturation Effect," *IEEE Trans. Ind. Informatics*, vol. 14, no. 5, pp. 1898–1908, 2018, doi: 10.1109/TII.2017.2759502.

[6] V. A. D. Faria, J. V. Bernardes, and E. C. Bortoni, "Parameter estimation of synchronous machines considering field voltage variation during the sudden short-circuit test," *Int. J. Electr. Power Energy Syst.*, vol. 114, no. July 2019, p. 105421, 2020.

[7] M. Micev, M. Ćalasan, D. S. Petrović, Z. M. Ali, N. V. Quynh and S. H. E. Abdel Aleem, "Field Current Waveform-Based Method for Estimation of Synchronous Generator Parameters Using Adaptive Black Widow Optimization Algorithm," in *IEEE Access*, vol. 8, pp. 207537-207550, 2020, doi: 10.1109/ACCESS.2020.3037510.

[8] M. Micev, M. Ćalasan, S. H. E. A. Aleem, H. M. Hasanien, and D. S. Petrović, "Two Novel Approaches for Identification of Synchronous Machine Parameters From Short-Circuit Current Waveform," *IEEE Trans. Ind. Electron.*, vol. 69, no. 6, pp. 5536–5546, 2022, doi: 10.1109/TIE.2021.3086715.

[9] M. Micev, M. Ćalasan, and M. Radulović, "Full Synchronous Machine Parameters Identification Based on Field and Armature Current During the Short-Circuit," *IEEE Trans. Ind. Appl.*, vol. 57, no. 6, pp. 5959–5968, 2021, doi: 10.1109/TIA.2021.3112141.

[10] J. Lidenholm and U. Lundin, "Estimation of hydropower generator parameters through field simulations of standard tests," *IEEE Trans. Energy Convers.*, vol. 25, no. 4, pp. 931–939, 2010, doi: 10.1109/TEC.2010.2064776.

[11] A. Mitra, A. Mohapatra, S. Chakrabarti, and S. Sarkar, "Online Measurement Based Joint Parameter Estimation of Synchronous Generator and Exciter," *IEEE Trans. Energy Convers.*, vol. 36, no. 2, pp. 820–830, 2021, doi: 10.1109/TEC.2020.3034733.

[12] M. Dehghani, M. Karrari, W. Rosehart, and O. P. Malik, "Synchronous machine model parameters estimation by a time-domain identification method," *Int. J. Electr. Power Energy Syst.*, vol. 32, no. 5, pp. 524–529, 2010, doi: 10.1016/j.ijepes.2009.07.010.

[13] Y. Xu, L. Mili, M. Korkali, and X. Chen, "An Adaptive Bayesian Parameter Estimation of a Synchronous Generator under Gross Errors," *IEEE Trans. Ind. Informatics*, vol. 16, no. 8, pp. 5088–5098, 2020, doi: 10.1109/TII.2019.2950238.

[14] Y. Li, J. Li, J. Qi, and L. Chen, "Robust cubature kalman filter for dynamic state estimation of synchronous machines under unknown measurement noise statistics," *IEEE Access*, vol. 7, pp. 29139–29148, 2019, doi: 10.1109/ACCESS.2019.2900228.

[15] A. Rouhani and A. Abur, "Constrained Iterated Unscented Kalman Filter for Dynamic State and Parameter Estimation," *IEEE Trans. Power Syst.*, vol. 33, no. 3, pp. 2404–2414, 2018, doi: 10.1109/TPWRS.2017.2764005.

[16] M. Hasni, O. Touhami, R. Ibtiouen, M. Fadel, and S. Caux, "Estimation of synchronous machine parameters by standstill tests," *Math. Comput. Simul.*, vol. 81, no. 2, pp. 277–289, 2010, doi: 10.1016/j.matcom.2010.05.010.

[17] M. Cisneros-González, C. Hernandez, R. Morales-Caporal, E. Bonilla-Huerta, and M. A. Arjona, "Parameter estimation of a synchronous-generator two-axis model based on the standstill chirp test," *IEEE Trans. Energy Convers.*, vol. 28, no. 1, pp. 44–51, 2013, doi: 10.1109/TEC.2012.2236433.

[18] M. A. Arjona, M. Cisneros-Gonzalez, and C. Hernandez, "Parameter estimation of a synchronous generator using a sine cardinal perturbation

and mixed stochastic deterministic algorithms," *IEEE Trans. Ind. Electron.*, vol. 58, no. 2, pp. 486–493, 2011.

[19] M. A. Arjona, C. Hernandez, M. Cisneros-Gonzalez, and R. Escarela-Perez, "Estimation of synchronous generator parameters using the standstill step-voltage test and a hybrid Genetic Algorithm," *Int. J. Electr. Power Energy Syst.*, vol. 35, no. 1, pp. 105–111, 2012.

[20] M. Giesbrecht and L. A. E. Meneses, "Detailed derivation and experimental validation of a method for obtaining load conditions for salient pole synchronous machine quadrature axis parameters determination," *IEEE Trans. Ind. Electron.*, vol. 66, no. 7, pp. 5049–5056, 2019, doi: 10.1109/TIE.2018.2866096.

[21] G. Hutchison, B. Zahawi, K. Harmer, S. Gadoue, and D. Giaouris, "Non-invasive identification of turbogenerator parameters from actual transient network data," *IET Gener. Transm. Distrib.*, vol. 9, no. 11, pp. 1129–1136, 2015, doi: 10.1049/iet-gtd.2014.0481.

[22] B. Zaker, R. Khalili, H. Rabieyan, and M. Karrari, "A new method to identify synchronous generator and turbine-governor parameters of a gas unit using a closed-loop model," *Int. Trans. Electr. Energy Syst.*, vol. 31, no. 11, p. e13110, Nov. 2021, doi: https://doi.org/10.1002/2050-7038.13110.

[23] E. L. Geraldi, T. C. C. Fernandes, A. B. Piardi, A. P. Grilo, and R. A. Ramos, "Parameter estimation of a synchronous generator model under unbalanced operating conditions," *Electr. Power Syst. Res.*, vol. 187, no. June, p. 106487, 2020, doi: 10.1016/j.epsr.2020.106487.

[24] K. K. Challa and G. Gurrala, "Dynamic State and Parameter Estimation of Synchronous Generator from Digital Relay Records," *Electr. Power Syst. Res.*, vol. 189, no. April, p. 106743, 2020, doi: 10.1016/j.epsr.2020.106743.

[25] T. L. Vandoorn, F. M. De Belie, T. J. Vyncke, J. A. Melkebeek, and P. Lataire, "Generation of multisinusoidal test signals for the identification of synchronous-machine parameters by using a voltage-source inverter," *IEEE Trans. Ind. Electron.*, vol. 57, no. 1, pp. 430–439, 2010, doi: 10.1109/TIE.2009.2031135.

[26] L. Beordo, E. P. T. Cari, T. G. Landgraf, and L. F. C. Alberto, "A comparative validation of a synchronous generator by trajectory sensitivity and offline methods," *Int. Trans. Electr. Energy Syst.*, vol. 27, no. 2, 2017, doi: 10.1002/etep.2255.

[27] O. Loyola-Gonzalez, "Black-box vs. White-Box: Understanding their advantages and weaknesses from a practical point of view," *IEEE Access*, vol. 7, pp. 154096–154113, 2019, doi: 10.1109/ACCESS.2019.2949286.

[28] A. G. Abro and J. M. Saleh, "ANN-based synchronous generator excitation for transient stability enhancement and voltage regulation," *Appl. Artif. Intell.*, vol. 27, no. 1, pp. 20–35, Jan. 2013, doi: 10.1080/08839514.2013.747369.

[29] I. A. Basheer and M. Hajmeer, "Artificial neural networks: fundamentals, computing, design, and application," *J. Microbiol. Methods*, vol. 43, no. 1, pp. 3–31, 2000, doi: https://doi.org/10.1016/S0167-7012(00)00201-3.

[30] M. Nørgaard, O. Ravn, N. K. Poulsen, L. K. Hansen," *Neural networks for Modelling and Control of Dynamic Systems*," 1st ed., Springer-Verlag, London, UK, 2000.

Mihailo Micev (S'19) received BSc and MSc degrees in electrical engineering from the University of Montenegro, Podgorica, in 2017, and 2020, respectively. He is currently a Teaching Assistant at the University of Montenegro and working towards his PhD thesis. His areas of research are switched reluctance machines, synchronous generators and regulation of electrical machines, as well as modelling and parameter estimation of electrical machines.

Martin Ćalasan (M'17) received the BSc, MSc, and Ph.D. degrees in electrical engineering from the University of Montenegro, Podgorica, in 2009, 2010, and 2017 respectively. He is currently working as an Assistant Professor in the Department of Power System and Automatics at the University of Montenegro. He serves as Secretary & Representative for Montenegro in IEEE Chapter Power & Energy (PE-31). His research interests include induction machine, switched reluctance generator, electrical braking, and excitation systems of synchronous generator and solar energy. He is a member of several international and national organizations and associations (Institute of Electrical and Electronics Engineers (IEEE), Conseil International des Grands Réseaux Electriques (CIGRE), and CIGRE CG KO). He also serves as the Secretary and a Representative for Montenegro in IEEE Chapter Power and Energy (PE-31).

Milovan Radulović (M'98) received the Ph.D. degree in electrical engineering from the Faculty of Electrical Engineering, University of Montenegro, Podgorica, Montenegro, in 2004. He is currently Full Professor with the Department of Automatic and Power System, Faculty of Electrical Engineering, University of Montenegro. His research interests include automation and control elements of power system, control and motion planning for mobile robot systems, as well as human–robot interaction and exoskeleton design and its application to rehabilitation.

Shady H. E. Abdel Aleem (M'12, SM'21) received B.Sc., M.Sc., and Ph.D. degrees in Electrical Power and Machines from the Faculty of Engineering, Helwan University, Egypt, in 2002, and the Faculty of Engineering, Cairo University, Egypt, in 2010 and 2013 respectively. Currently, he is an Associate Professor at the Department of Electrical Engineering and Electronics, Valley Higher Institute of Engineering and Technology, Science Valley Academy, Qalubia, Egypt. He is the Vice Dean for Graduate Studies and Scientific Research. Also, he is a consultant of power quality studies in ETA Electric Company, Egypt. His research interests include harmonic problems in power systems, power quality, renewable energy, smart grid, energy efficiency, optimization, green energy, and economics.

Dr. Shady is the author or co-author of many refereed journals and conference papers. He has published 180 plus journal and conference papers, 18 plus book chapters, and 8 edited books with the Institution of Engineering and Technology (IET) (2), Elsevier (3), Springer (1) and InTech (2). He was awarded the State Encouragement Award in Engineering Sciences in 2017 from Egypt. He was also awarded the medal of distinction from the first class of the Egyptian State Award in 2020 from Egypt. Dr. Shady is a senior member of the Institute of Electrical and Electronics Engineers (IEEE). Dr. Shady is also a member of the Institution of Engineering and Technology (IET). He is an Editor/Guest Editor/Associate Editor for the *International Journal of Renewable Energy Technology, Vehicle Dynamics*, *IET Journal of Engineering, Energies, Sustainability, Technology and Economics of Smart Grids and Sustainable Energy*, and *International Journal of Electrical Engineering Education*.

Hany M. Hasanien (M 09, SM 11) received his B.Sc., M.Sc. and Ph.D. degrees in Electrical Engineering from Ain Shams University, Faculty of Engineering, Cairo, Egypt, in 1999, 2004, and 2007, respectively. From 2008 to 2011, he was a Joint Researcher with Kitami Institute of Technology, Kitami, Japan. From 2012 to 2015, he was Associate Professor at College of Engineering, King Saud University, Riyadh, Saudi Arabia. Currently, he is Professor at the Electrical Power and Machines Department, Faculty of Engineering, Ain Shams University. His research interests include modern control techniques, power systems dynamics and control, energy storage systems, renewable energy systems, and smart grid.

Prof. Hasanien is an Editorial Board Member of *Electric Power Components and Systems Journal*. He is Subject Editor of IET Renewable Power Generation, Ain Shams Engineering Journal and Electronics MDPI. He has authored, co-authored, and edited three books in the field of electric machines and renewable energy. He has published more than 150 papers in international journals and conferences. His biography has been included in *Marquis Who's Who in the*

world for its 28th edition, 2011. He was awarded Encouraging Egypt Award for Engineering Sciences in 2012. He was awarded Institutions Egypt Award for Invention and Innovation of Renewable Energy Systems Development in 2014. He was awarded the Superiority Egypt Award for Engineering Sciences in 2019. Currently, he is Editor in Chief of Ain Shams Engineering Journal and is the IEEE PES Egypt Chapter Chair.

Ahmed F. Zobaa (M'02_SM'04) received B.Sc. (Hons), M.Sc., and Ph.D. degrees in Electrical Power and Machines from Cairo University, Egypt, in 1992, 1997, and 2002, respectively. Between 2007 and 2010, he was a Senior Lecturer in Renewable Energy at University of Exeter, U.K. He was also an Instructor at Cairo University between 1992 and 1997, a Teaching Assistant between 1997 and 2002, an Assistant Professor between 2003 to 2008, an Associate Professor from 2008 and 2013, where he has also been a professor (on leave) since December 2013. Currently, he is a Reader in Power Systems, and a Full Member of the Institute of Energy Futures at Brunel University London, U.K. His main areas of expertise are power quality, (marine) renewable energy, smart grids, energy efficiency, and lighting applications. Dr. Zobaa is Editor-in-Chief for the *International Journal of Renewable Energy Technology*, *International Journal of Electrical Engineering & Education,* and *Technology and Economics of Smart Grids and Sustainable Energy*. He is also an Editorial Board member, Editor, Associate Editor, and Editorial Advisory Board member for many international journals. He is a registered Chartered Engineer, Chartered Energy Engineer, European Engineer, and International Professional Engineer, and is a registered member of the Engineering Council U.K., Egypt Syndicate of Engineers, and the Egyptian Society of Engineers. He is a Senior Fellow of the Higher Education Academy of U.K., and a Fellow of the IET, the Energy Institute of the U.K., the Chartered Institution of Building Services Engineers, the Institution of Mechanical Engineers, the Royal Society of Arts, the African Academy of Science, and the Chartered Institute of Educational Assessors. He is a senior member of the IEEE, and is a member of the International Solar Energy Society, the European Power Electronics and Drives Association, and the IEEE Standards Association.